

Chloride Threshold Levels in Clad 316L and Solid 316LN Stainless Steel Rebar

Michael F. Hurley, John R. Scully

Center for Electrochemical Science and Engineering
Department of Materials Science and Engineering
University of Virginia
Charlottesville, VA 22904-4745

ABSTRACT

Initiation of corrosion on reinforcing bars occurs when a critical chloride concentration is achieved. A universal value for the chloride concentration that causes depassivation has not been agreed upon for carbon steels due to a variety of experimental factors. The chloride threshold depends on the rebar material, rebar surface condition, testing environment, method of detection, definition of depassivation, and method of expression of results. However, most data for carbon steel points to a Cl^-/OH^- molar ratio <1 . The chloride threshold for stainless steel clad rebar is unknown. The chloride threshold for solid 316LN stainless steel, 316L stainless steel clad, and carbon steel rebar was investigated through current monitoring during potentiostatic polarization with comparison to open circuit potentials (in a saturated $\text{Ca}(\text{OH})_2 + \text{NaCl}$ in glass sand bead mixture). Solid 316LN stainless steel rebar was found to have a much higher chloride threshold (i.e. threshold Cl^-/OH^- ratio >24) than carbon steel at all potentials investigated (-200, 0.00, and +200 mV vs. SCE). The chloride threshold for 316L clad rebar was highly dependent on defects and the method used to seal the cut end, which exposes the carbon steel core. At best, it was similar to that of solid stainless steel and at worst, it was less than that of carbon steel rebar, owing to elevation in potential due to galvanic coupling between a defective clad layer and the exposed carbon steel core.

INTRODUCTION

In many parts of U.S., where de-icing salts are used in the winters, corrosion of reinforcing steel bars is the prevalent cause of the deterioration – often prematurely – of

concrete bridges. For analysis of the life-cycle cost of any concrete bridge member exposed to chloride intrusion, the service life is considered to be the sum of the corrosion initiation phase and the propagation phase, as illustrated in Figure 1.

The corrosion initiation phase is the time required, from the day the structure is put into service, for chloride ions to permeate from its surface and through the pores in the concrete to accumulate in the concrete surrounding the bars eventually to a concentration sufficient to initiate corrosion on the bars, which is known as the chloride threshold level. If no cracks are present – especially those that are wider than 0.3 mm (0.01 in.)^[1,2] – the length of this phase is a function of the permeability of the concrete, the concrete cover, the type of cementitious materials used, and the corrosion resistance of the bars. However, when wide cracks are present in the concrete deck, then corrosion resistance of the bars becomes the only factor that has any practical influence on the corrosion initiation phase. The propagation phase is the time required for corrosion on the bars to propagate across the structure to the point at which either the load bearing capacity of the structural elements becomes inadequate, or it becomes more economical to replace the elements than to keep repairing the resulting corrosion-induced concrete damage. Since carbon steel bars, either bare or epoxy-coated, have been up until now the only bars available, the length of this phase has been considered to be influenced only by the concrete cover, the properties of the concrete, and the local economics of concrete repair.

Prompted by rapidly rising highway construction costs, bridge designers have recently raised their design goal for new concrete bridges from 50-years to at least 75-years service life for regular bridges and 100-years service life for major bridges. To meet this goal, new reinforcing bars that are significantly more corrosion resistant than the carbon steel and, in many aspects, more forgiving than the widely used epoxy-coated carbon steel bars would be needed. One class of materials meeting these objectives is stainless steel and/or stainless steel cladding over A615M carbon steel (clad thickness of 1-2 mm) as shown in Figure 2. However, the chloride threshold level of these new materials is unknown.

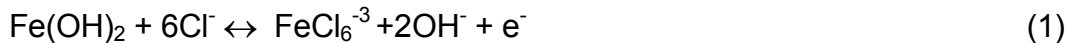
BACKGROUND

Chloride Induced Corrosion

Reinforcing bars embedded in concrete undergo depassivation and subsequent corrosion due to carbonation, chloride ingress, or a combination of both. The time until either of the two mechanisms involved leads to depassivation is considered the initiation stage and the ensuing active corrosion period is known as the propagation stage.^[3] Carbonation is controlled by the diffusion of CO₂ through concrete. CO₂ molecules react with species present in the concrete such as solid calcium hydroxide, alkali, and calcium ions to lower the pH of the pore solution, causing depassivation. Corrosion initiation by carbonation is considered to be only a function of the concrete cover and quality. Hence it will not be discussed further.

Chloride induced depassivation of steel is thought to be caused by the interference of chloride ions in the formation of the naturally occurring passive film, enabled by the presence of OH⁻ ions in the alkaline pore solution. The oxide film afforded by steel in the presence of sufficient OH⁻ ions develops as iron is converted to ferrous ions. These ions are converted to form either ferrous (Fe²⁺) or ferric (Fe³⁺) oxide (also known as γ -FeOOH).^[4] Ferrous and Ferric oxides are not protective at pH levels less than approximately 11.5.^[5] Although γ -FeOOH is the

more stable of the two oxides, it forms slowly over time as the ferrous oxide is converted into ferric oxi-hydroxide, and observed by the presence of a passive corrosion current density. Because this conversion is never totally complete chloride ions may compete with the conversion of $\text{Fe}(\text{OH})_2$ to $\gamma\text{-FeOOH}$ by the following reaction:



The chloride complex formed in eqn. 1 is soluble in the surrounding pore solution and, therefore, does not provide protection against corrosion to the rebar surface. Pore solutions containing sufficient chloride concentrations will promote localized areas of depassivation on the rebar surface where the ferrous oxide has not been converted to $\gamma\text{-FeOOH}$ even if the pore solution pH is above 11.5.

There is general agreement in the literature that chloride ions lead to depassivation but the exact mechanism is not well understood. One theory is that dissolved oxygen predominately favors the $\gamma\text{-FeOOH}$ conversion reaction and therefore, localized pitting attack caused by sufficient chloride ion concentration will preferentially occur at regions of low dissolved oxygen content.^[4] According to the adsorption theory, the passive film becomes unstable when chloride ions replace oxygen ions held within the passive film, causing a difference in electrochemical potential across the film.^[7] According to the oxide film theory, the oxide layer has inherent defects and pores. Chloride ions penetrate the oxide layer at these defects due to the dissolution of the more reactive species in the oxide layer.^[5] The latter two theories more likely apply to stainless steel with a mixed Cr-Fe bound oxide. Chloride adsorption and oxide penetration are promoted by raising the electrochemical potential. Thus, higher oxygen levels would be detrimental. Regardless, initiation occurs in either of these latter two mechanisms once sufficient accumulation of chloride ions has depressed the critical pitting potential of the passive steel rebar to below that of the OCP.^[6]

All of these theories suggest that initiation is a localized phenomenon caused by sufficient amount of chloride ions. The critical chloride content or chloride threshold concentration is the concentration of Cl^- ions which is sufficient to cause active corrosion or induce pitting. The chloride threshold is unknown for clad stainless steel. Moreover, a standardized definition for both an active corrosion condition for rebar in concrete and a universal expression for chloride threshold content has not been adopted. This issue will be addressed in the following section.

Defining the Active Corrosion State and an Expression for the Threshold Chloride Content

One problem with identifying a unique value for the threshold chloride content stems from ambiguity in quantitatively defining when active corrosion occurs as well as when pitting initiation and stabilization occur. Differences in experimental technique and setup from separate authors have contributed to the lack of agreement in defining depassivation of rebar in concrete. Some authors have defined active corrosion when a certain shift in the OCP of the rebar occurs.^[8,9] Other authors have used a more qualitative approach, identifying depassivation with the visual appearance of rust spots on the steel surface^[8-11] Lastly, others have used certain level in the corrosion rate at open circuit to define depassivation.^[11-17] Of these, some use a direct measurement of the corrosion current^[11-15,17] or the detection of the increase in the galvanic current^[16] as the indicator of active corrosion. The use of the polarization resistance technique

as a means to measure corrosion rate has also been used to identify a loss of passivity.^[18,19] More recently a generally agreed upon value of the corrosion current density ($i_{\text{corr}} > \sim 0.1\text{-}0.2 \mu\text{A}/\text{cm}^2$) has been considered to signify active corrosion of steel in concrete. This condition is further complicated by the fact that some tests have been conducted at open circuit potential, while others have been conducted under potentiostatic condition^[20,21] or by anodic polarization.^[9,22] A critical unresolved issue is the level of polarization. Plain carbon steel is often tested at OCP while stainless steel is tested when anodically polarized.

Further defining active corrosion of rebar in steel requires an indication of the time involved. From a practical standpoint, defining the transition from passive to active corrosion requires that the conditions favoring depassivation remain present with time. Because of the stipulation that depassivating conditions must remain over time, certain definitions of active corrosion are less reliable. Observation of the formation of oxides via the visual inspection technique may not necessarily indicate steady active corrosion or conversely significant accumulation of oxides may not occur until some time after the shift to active corrosion. Likewise, during OCP monitoring a shift in E_{corr} may not be detected upon depassivation or may not necessarily mean significant depassivation, depending on experimental test conditions.

Although it is generally agreed that a unique critical concentration of chloride ions that leads to depassivation exists; there is little agreement on a exact quantitative amount of chloride required for depassivating carbon steel. The concentration of chloride that causes depassivation relies heavily on other variables such as oxygen concentration, pH, rebar surface conditions, presence of others ions in the pore solution and various concrete properties including; type of aggregate, concrete additives, mix design, moisture level, and air content. Chloride threshold values published in the literature are generally based upon tests conducted in three different types of experimental setups. The three typical environments are; rebar cast in concrete, rebar cast in mortar specimens, and rebar in synthetic pore solution(s). The experimental method chosen has led to different expressions for the presentation of the chloride threshold content.

Results from tests conducted in concrete or mortar are commonly presented as a total chloride content expressed relative to the weight of concrete. This is a relatively simple way to express the data and has been documented in standards.^[23,24] Despite the ease of using this method, it may not be adequate enough to be applied to all chloride threshold data. The concrete/rebar interface is very complex and presenting the data simply as total chloride by weight of concrete can lead to spread in the data due to experimental variables inherent with working with concrete. For example the influence of bound chloride, precipitated calcium hydroxide, and concrete water content have been the subject of some debate.^[25-27] Usually soluble Cl^- is the culprit in global depassivation or FeCl_x formation on carbon steels.

Chloride binding is the interaction between porous concrete and chloride ions which results in their effective removal from the pore solution. A proportion of the chloride present in the concrete mix becomes bound in all cements. One important variable concerning the amount of chloride binding which occurs, is the C_3A content of the cement.^[26] A greater amount of chloride becomes bound with increasing C_3A content. This occurs by the formation of a relatively insoluble hydration compound called Friedel's salt ($\text{C}_3\text{A}\cdot\text{CaCl}_2\cdot 15\text{H}_2\text{O}$).^[5] Other factors including silica fume, granulated blast furnace slag cement replacement, pore solution hydroxyl concentration, cation of the chloride salt, and the water/cement also effect chloride binding capacity.^[27] The effect of chloride binding on the chloride threshold is unresolved. Chloride threshold results have also been presented as free chloride (chloride ion concentration in pore

solution only) or as a chloride to hydroxyl ion ratio. Presentation of data via these two approaches takes into account the hypothesis that only unbound chloride ions contribute to the corrosion activity of steel in concrete. However, it has been shown that presenting the data this way does not decrease the range of chloride threshold values presented, in some cases actually the spread is greater.^[26,27] One possible explanation of this is the effect of the water/cement ratio on chloride binding behavior. A non-linear relationship has been observed between free and total chloride content as a function of water content in the mix design, see Figure 3. Also, the resistivity of the concrete and the amount of precipitated $\text{Ca}(\text{OH})_2$ may be effected by a change in moisture content. Both of these also effect the corrosion behavior of the rebar and, therefore, the chloride threshold.

Only chloride threshold tests conducted with embedded rebar in concrete or mortars have been considered up until this point. Synthetic pore solution tests have been used for simulating the concrete environment. Using synthetic pore solution tests yields less spread in the chloride threshold data for carbon steel bars (Figure 4), possibly by the elimination of many variables associated with the concrete matrix and the concrete/rebar interface. Greater control is gained over the Cl^- to OH^- ratio. Although, it can be seen that the results from simulated pore solution tests are more conservative than in concrete tests.^[28] A part of the difference between solution and concrete testing can be attributed to the presence of $\text{Ca}(\text{OH})_2$ crystals at the steel concrete interface. $\text{Ca}(\text{OH})_2$ crystals can restrain a pH drop at the interface and dissolution of $\text{Ca}(\text{OH})_2$ crystals during active corrosion has been observed.^[28] The $\text{Ca}(\text{OH})_2$ crystals essentially provide an alkali reservoir that can prolong a high pH, keeping the rebar in the passive range. Although testing in simulated pore solutions may provide results that are more precise than in concrete or mortars, they are more conservative.

In comparison to carbon steel, stainless steel rebar (containing 18% Cr) is expected to be passive through a much broader range of pH's, due to thermodynamic considerations when Cr is added to Fe-based alloys.^[29] Also, stainless steel has much greater resistance to localized corrosion compared to carbon steel, and would be expected to have a much longer initiation stage prior to depassivation.

A summary of chloride threshold results for carbon steel and stainless steel are presented in Tables 1a and 1b, after Glass^[30] and Alonso et al.^[18] This summarizes different experiments in all three of the common chloride threshold test environments. The methods of definition of depassivation and expression of results are also presented. The results for steel generally agree that Cl^-/OH^- threshold < 1 exist for solution tests. However, some results in concrete suggest $\text{Cl}^-/\text{OH}^- < 4$. Kurtis and Mehta^[5] argue that mineral scales in concrete improve passivity and thus raise Cl^- threshold when tests are conducted in concrete.

A chloride threshold is found for carbon steel in mortar and concrete (Table 1a) while, in contrast, stainless steel exposed in chloride contaminated concrete showed no signs of active corrosion after 22 years. The results indicate a higher chloride threshold level in stainless steel compared to carbon steel when tests conducted in aqueous solutions are compared to those for carbon steel. Stainless steel also exhibited a higher chloride threshold as the pH was raised. However, little is known about chloride thresholds for clad stainless steel or solid stainless steel tested in a simulated pore solution at pH of 12.6 or greater. This study investigates clad, defective clad and solid 316L stainless steels.

Table 1a. Survey of existing data of the chloride threshold concentration to initiate active corrosion on carbon steel rebar (literature data %wc = percentage chloride detected by weight of cement). After Glass^[30]Alonso^[18].

| Carbon Steel (Conditions) | Reference | Environment | Threshold Values or Ranges | | | Depassivation detection method |
|--|---------------------------|------------------------------|--------------------------------|--------------------------------|----------------------------------|---|
| | | | Free Cl ⁻ (% wc) | Total Cl ⁻ (%wc) | Cl ⁻ /OH ⁻ | |
| Solutions simulating concrete | Hausmann [8] | Solution | | | 0.60 | Shift in E _{corr} |
| Solutions simulating concrete | Gouda [9] | Solution | | | 0.35 | Anodic polarization, shift in E _{corr} , visual inspection |
| Steel in alkaline solutions with chlorides | Goni and Andrade [13] | Solutions | | | 0.25-0.8 | Avg. corrosion rate |
| Mortar suspensions | Gouda and Halaka [22] | OPC BFSC | | 2.42 1.21 | | Anodic polarization |
| Cements with high or low alkali content | Petterson [12,15,31] | Mortars 80% RH 100% RH | | 0.6-1.8 0.5-1.7 | 2.5-6.0 1.7-2.6 1.7-2.6 | Corrosion rate |
| Brit. OPC and Sp. BFSC (Cl ⁻ added as admixture) | Andrade and Page [17] | OPC BFSC | | | 0.15-0.69 0.12-0.44 | Corrosion rate |
| Three OPC Mortar (external chloride) | Hansson and Sorenson [20] | 100% RH 50% RH | | 0.6-1.4 | | Corrosion rate, potentiostatic |
| Concrete slabs stored in 10% seawater | Petterson [12,15,31] | Concrete | | | 1.8-2.9 | Corrosion rate |
| Concrete (external chloride) | Lambert et al. [14] | Concrete | | | 3.0 | Corrosion rate |
| Concrete with added Cl ⁻ | Gouda and Halaka [22] | OPC BFSC | | 3.04 1.01 | | Anodic polarization |
| No pre-cleaning bars | Gouda and Halaka [22] | OPC | | 0.6 | | Anodic polarization |
| Cl ⁻ added as admixture Med. Strength concrete High strength concrete High strength concrete + supplement High strength concrete + supplement + fly ash | Kayyali and Haque [32] | Concrete | 1.15 0.85 0.80 0.45 | | | Assuming threshold Cl ⁻ /OH ⁻ = 0.6 |
| Cement with different C ₃ A content C ₃ A = 2.43% C ₃ A = 7.59% C ₃ A = 14.00% | Hussain et al [33] | Concrete | 0.14 0.17 0.22 | 0.35 0.62 1.0 | | Assuming threshold Cl ⁻ /OH ⁻ = 0.3 |
| Concrete with admixed Cl ⁻ and externally exposed to Cl ⁻ | Schiessl and Breit [16] | | | 0.5-1 1-1.5 1-1.5 | | Macrocell currents |
| Concrete prisms at marine exposure | Thomas et al. [10] | Concrete | | 0.5 | | Visual observation, mass loss |
| Reinforced concrete prisms with fly ash at marine exposure Fly ash = 0% Fly ash = 15% Fly ash = 30% Fly ash = 50% | Thomas [34] | Concrete | | 0.70 0.65 0.50 0.20 | | Mass loss |

| | | | | | | |
|--|--------------------|------------------------|-----------|-----------|-----------------------|--|
| Concrete slabs with added Cl ⁻ to various exposure conditions | Hope and Ip [11] | OPC | | 0.1-0.19 | | Corrosion rate, visual inspection, mass loss |
| Simulated pore solution | Li and Sagues [19] | pH = 12.6 pH = 13.5 | | | 0.25-0.7 1.05-1.25 | Shift in E _{corr} , polarization resistance |
| Simulated pore solution and mortars | Alonso et al. [18] | Solution Mortar | 1.24-3.08 | 0.39-1.16 | 0.25-0.8 1.17-3.98 | Various |

Table 1b. Summary of reported chloride threshold values for solid stainless steel rebar

| Stainless Steel (Conditions) | Reference | Environment | Threshold Values or Ranges | | | Depassivation detection method |
|--|------------------------|----------------------------------|-----------------------------|-----------------------------|----------------------------------|--|
| | | | Free Cl ⁻ (% wc) | Total Cl ⁻ (%wc) | Cl ⁻ /OH ⁻ | |
| Concrete prisms 302,315,316 bar | Cox and Oldfield [35] | Concrete | > 3.2% | | | Visual inspection after 22 years showed no signs of active corrosion |
| Ca(OH) ₂ based pore solutions 304, 304L,316, 316L | Bertonlini et al. [21] | pH = 9 pH = 12.6 pH = 13.9 | | | 1-4 > 2 > 8 | Corrosion rate, potentiostatic hold at +200 mV (vs. SCE) |

OPC = ordinary portland cement, BFSC = Blast furnace slag cement, RH = Relative humidity

METHODS OF INVESTIGATION

Materials and Experimental Setup

In order to determine the possible benefits from a chloride threshold corrosion standpoint of using a novel type of rebar, electrochemical tests were performed on three types of rebar, carbon steel AISI A615M, solid stainless steel 316LN, and stainless steel clad. The composition of the rebars is presented in Table 2. The plain steel and solid stainless steel bars were size #5 (diameter ≈ 17.5 mm). The 316L stainless steel clad bar was size #6 (diameter ≈ 20 mm, clad layer 1-2 mm thick, see Figure 2). Electrochemical testing was performed in a custom built electrochemical cell which allowed testing of the rebar in a vertical orientation. Specimen preparation will be discussed in the following text.

Vertical cell test samples were prepared from ≈ 70 mm sections of rebar. One end of each test piece was drilled and tapped with ≈ 40 mm piece of 1040 threaded rod, shown in Figure 5. This established electrical contact with the sample and served as a sample holder when threaded with a #3 rubber stopper. Copper paste was added at the threaded interface between the threaded rod and the rebar to enhance electrical contact. The threaded rod was secured to the rebar with a stainless steel hex nut. The vertical cell enabled testing of the rebar surface that is exposed during service conditions.

Aside from the cleaning procedure and end-capping, the surface condition of the rebar samples was essentially as-received. Each rebar specimen was washed, degreased and ultrasonically cleaned in acetone, rinsed with deionized water, dried at room temperature, and stored in a vacuum jar. Prior to testing, the hex nut and the tapped end of the sample were covered with an anti-crevice mask (MPM Masking 3500) to prevent electrolyte contact and unwanted secondary electrochemical reactions. The procedure for sealing the exposed end (cross section at the end of the rebar) will be addressed in the following section since the results depended on the method used to seal the exposed end.

Table 2. Composition in wt. % of rebars used in study.

| Rebar | C | P | S | Mn | Si | Cr | Ni | Mo | Cu | Ti | N ₂ | Fe |
|--------------------|-------|-------|-------|-------|-------|-------|--------|-------|-------|-------|----------------|------|
| Plain Carbon Steel | 0.43 | 0.007 | 0.038 | 1.11 | 0.22 | 0.03 | 0.11 | <.01 | 0.37 | -- | -- | Bal. |
| Solid 316LN SS | 0.026 | 0.022 | 0.015 | 1.486 | 0.447 | 17.84 | 11.775 | 2.848 | 0.253 | 0.006 | 0.2175 | Bal. |
| 316L Clad Layer* | 0.03 | 0.045 | 0.03 | 2 | 0.075 | 16.5 | 10-14 | 2-3 | | | | |

*over plain carbon steel

Vertical cell experiments relied on a custom built three-electrode electrochemical cell. The modified cell design was used for two reasons: to avoid unwanted crevice attack which occurs with specimen/Teflon washer contact on a flat cell, and to perform accelerated testing on the rebar surface which is actually exposed during service. With a conventional flat cell only the cross-sectional face of the cut rebar is exposed. A 1-liter, acrylic jar was sealed with a Teflon lid fitted with a rubber O-ring gasket. The Teflon lid contained openings for a reference electrode, rubber stopper mounted rebar specimen, and a platinum-coated rod, which held the cylindrical counter electrode. A saturated calomel reference electrode (SCE) with a Luggin capillary probe was used in all experiments with the sensing tip approximately 10 mm from the sample. The cylindrical counter electrode was constructed from platinized niobium mesh, 305 mm by 25 mm (effective surface area was much larger), spot welded to a platinum coated titanium rod. The working electrode surface area was approximately 40 cm².

The electrolyte solution used in this investigation was saturated Ca(OH)₂ (pH 12.6). All solutions were prepared with reagent grade chemicals and dionized water of 18.2 MΩ resistivity. Ottawa Sand (ASTM-C109) and glass beads (diameter 6 mm and 3 mm) were added to this test solution for certain tests with the dual purpose, to simulate in service rebar/concrete-aggregate crevice corrosion conditions and to enable rapid examination of surfaces after testing. Two different glass bead sizes were used, 6 mm and 3 mm, to mimic the use of fine (< 4.75 mm in diameter) and course aggregates (> 4.75 mm in diameter) in concrete. The ratio of 6 mm beads to 3 mm beads was approximately 3:1, and the additional volume was filled with Ottawa sand.

Electrochemical Testing

Potentiostatic polarization and OCP monitoring were used to find a threshold chloride content for the three types of rebar tested: carbon steel, 316LN stainless steel, and 316L clad over a carbon steel core. The potentiostatic tests were carried out at three potentials: -200 mV, 0 mV, and +200 mV (all potentials vs. SCE). All tests were carried out in Sat. Ca(OH)₂, with chloride additions made using NaCl. Samples were in the vertical cell configuration with Sat. Ca(OH)₂ and polarized to the selected potential. After an initial 24 hours, chloride additions were made every 24 hours until the cut off current density of 2-3 μA/cm² was exceeded. Upon reaching the threshold current density, the test was terminated. The threshold chloride content was noted as the cumulative amount of chloride that had been added throughout the duration of

the test (see Figure 4). Chloride additions were made every 24 hours in order to give the system sufficient time to stabilize.

Experiments were also carried out to obtain a reliable open circuit potential (OCP) and tests were run to find corrosion potentials for carbon steel, solid stainless steel, and stainless steel clad rebar (intact as well as with defects in the clad layer). These tests were performed in both the vertical cell with simulated pore solution as well as in chloride contaminated concrete.

RESULTS

Chloride Threshold Levels

Chloride threshold experiments under potentiostatic polarization indeed displayed net anodic current, which increased with time upon step chloride additions. An example of typical results for carbon steel is shown in Figure 6. A shift in current density to above $2\text{-}3 \mu\text{Amps/cm}^2$ was used as the criteria for detecting the transition to active corrosion. In each test the chloride concentration that caused the shift to active corrosion was noted as the chloride threshold content and presented as the ratio of chloride ion to hydroxyl ion concentration.

A plot comparing reported chloride threshold values of carbon steel to those of solid stainless steel rebar are presented in Figure 7. All tests on stainless steel were conducted under potentiostatic polarization to +200 mV vs. SCE. This is seen as a conservative upper limit for the open circuit potential of stainless steel rebar in concrete. For rebar in concrete exposed to atmospheric conditions the free corrosion potential typically ranges between -150 to $+50$ mV vs. SCE.^[21] All of the solid stainless steel bars had chloride threshold values of Cl^-/OH^- exceeding 24 whereas values for carbon steel were all below 1, regardless of investigators. This increase in chloride threshold is expected based on the pitting resistance equivalency number (PREN) of stainless steel (between 20-30 depending on grade) when it is compared to carbon steel (less than 1). This number is solely a function of Cr, Mo, and N composition of the stainless steel and has been used to predict the localized corrosion resistance of stainless steels.^[36]

The chloride threshold for stainless steel clad rebar compared to that of solid stainless steel and carbon steel (all conducted at potentiostatic holds of +200 mV) is presented in Figure 8. The chloride threshold for clad rebar shows a strong dependence on the method and quality of sealing the exposed end (see Figure 8). The clad sample with the end exposed, that is with the cross sectional face on bottom exposing the carbon steel core, showed a chloride threshold equal to that of plain carbon steel. End sealing with a 316L weld yielded little increase in the threshold value, $\text{Cl}^-/\text{OH}^- \approx 4$, this was surprisingly low compared to that of solid stainless steel. In the case of the 316L welded end, active corrosion was almost exclusively limited to the radial surface on the rebar that came in contact with the weld, as opposed to the down facing cross sectional area. In order to avoid any possible end weld-rebar interface effects, end sealing with epoxy was performed. End capping with epoxy yielded a substantially higher chloride threshold compared to 316L end welding or an exposed end. Some difference is seen between two attempts at epoxy end sealing. In both attempts when active corrosion occurred, corrosion products were seen under or near the carbon steel-rebar/end-epoxy interface. Figure 9 shows attack on the carbon steel core of the first epoxy end sealed test, post testing with the epoxy removed. Hence, clad rebar with sealed ends often exhibited a

chloride threshold reflecting the quality of the seal at the cut end. Testing was also performed on clad stainless steel bends that did not involve cut ends. In this case, the chloride thresholds approached solid stainless steel. Values of Cl^-/OH^- greater than 15 were obtained at +200 mV vs. SCE.

The effect of potential on the chloride threshold value was also explored. Chloride threshold determination tests were performed under potentiostatic polarization at the following potentials; -200, 0, and +200 mV vs. SCE (Figure 10). Carbon steel shows little effect of applied potential on the chloride threshold, although a drop is seen at 0 V vs. SCE and above. Solid stainless steel chloride threshold values are much higher than those of carbon steel at all potentials. Solid stainless steel shows a decrease in chloride threshold at a potential of +200 mV vs. SCE. There is no exact number for the chloride threshold for solid stainless steel at and below 0 V vs. SCE. This is due to the fact that the test solution had become saturated with NaCl prior to current increase above 2-3 $\mu\text{Amps}/\text{cm}^2$. Therefore the chloride concentration could not be increased. A conservative approach puts the threshold value at the NaCl saturation point.

Open Circuit Potentials

It is of interest to compare the OCP of the different rebars in concrete to the chloride threshold obtained at various potentials in order to determine which potential dependent chloride threshold best describes the situation in concrete. Open circuit potential values for the three types of rebar tested are presented in Figure 11 (conducted in chloride contaminated concrete) and Figure 12 (conducted in simulated concrete with Ottawa sand and glass beads). The dependence of open circuit potential on rebar material can be seen. The carbon steel open circuit potential is much more negative than that of solid stainless steel, while values for stainless steel clad rebar are between those of stainless steel and carbon steel. Values in the $\text{Ca}(\text{OH})_2$ solution are similar to those in concrete. It can be seen that the chloride threshold of stainless steel remains high even at an OCP of +200 mV vs. SCE. In contrast, the chloride threshold of carbon steel is low even at an OCP of -500 mV vs. SCE. A detrimental situation is created by exposure of stainless steel clad rebar with a cut end. Here the OCP can remain high due to galvanic coupling between stainless steel cladding and the exposed carbon steel core, but the chloride threshold at the exposed surface drops to that of carbon steel.

DISCUSSION

Relationship Between Chloride Threshold and Potential Threshold

Stainless steel has a much higher chloride threshold (Cl^-/OH^- molar ratio > 100) than carbon steel (Cl^-/OH^- molar ratio approximately 1) for tests conducted at 0 mV and -200 mV vs. SCE in solutions. These results are likely conservative since the $\text{Ca}(\text{OH})_2$ solution may be more aggressive than concrete. The effect of mineral scales (in concrete tests) in elevating chloride threshold values is not likely seen in the simulated pore solution tested here. Moreover, stainless steel is already passivated by a Cr-Fe rich oxide. Therefore, it is reasonable to predict that mineral scale effect in concrete may provide limited additional benefit for stainless steel compared to that seen with carbon steel. However, the added buffering capability of precipitated $\text{Ca}(\text{OH})_2$ in concrete may still enhance chloride thresholds for stainless steel.

The chloride threshold obtained in potentiostatic tests on solid stainless steel represent the condition when the applied potential (E_{app}) or the potential the test is conducted at, exceeds a chloride dependent critical threshold potential (E_{thres}) for chloride induced pitting such as the repassivation potential.

Localized corrosion occurs if: $E_{app} \geq E_{thres}$

The critical potential or repassivation potential for stainless steel is often a function of chloride activity as expressed by: $E_{thres} = A - B \cdot \log[Cl^-]$ where A and B are constants.^[38] Thus, increases in chloride concentration lower E_{thres} to the point where the condition $E_{app} \geq E_{thres}$ occurs. Once this potential is exceeded localized corrosion events will propagate. Potentiostatic holds enable determination of chloride thresholds for stainless steel when NaCl is added in steps. E_{app} may then be compared to E_{ocp} . Conversely, it is unlikely that potentiodynamic scans would provide a reliable indication of chloride thresholds^[6] in stainless steel because of the long incubation times associated with the initiation of chloride induced attack.

Influence of Chloride Threshold on Relative Initiation Time

Given the difference in chloride thresholds between plain carbon steel and stainless steel, it is of interest to comment on the relative extension of the time until initiation of corrosion when stainless steel or stainless steel clad rebar is used instead of uncoated rebar steel. In order to conduct such a comparison, Fickian diffusion of Cl^- into concrete must be considered. Given the increase in Cl^- threshold expressed as Cl^-/OH^- molar ratio from molar ratio 1 for plain carbon steel to Cl^-/OH^- of 100 for solid stainless steel, the following question can be asked. How long does it take for the Cl^-/OH^- molar ratio in the concrete pore solution adjacent to an embedded rebar to reach the chloride thresholds described? Such a calculation can be performed assuming diffusion of Cl^- into concrete to the depth of the rebar from the concrete surface by purely concentration gradient driven diffusion.^[4,5,39-41] Using a mathematical solution to the diffusive transport equation yields equation (2). Equation 2 describes the Cl^-/OH^- ratio as a function of depth and time assuming a constant surface concentration and transport into a semi-infinite medium.

$$C(x,t) = C_o \cdot \{1 - \text{erf}[x / (D_{eff} \cdot t)^{1/2}]\} \quad (2)$$

Here $C(x,t)$ is the chloride concentration at depth x and time t , C_o is the surface concentration, and D_{eff} is the effective diffusion coefficient. Assuming a high quality concrete ($w/c = 0.4$) at a temperature of 22°C and a constant concrete cover of 5 cm, such a relative calculation has been performed. Using D_{eff} of $3 \times 10^{-8} \text{ cm}^2/\text{sec}$ ^[4] and cover depth, $x = 5 \text{ cm}$, it can be seen that it takes approximately 2.3 times longer to reach a Cl^-/OH^- ratio of 10 compared to 1 at a depth of 5 cm. Other examples indicate that it takes approximately 50 times longer to reach a Cl^-/OH^- ratio of 100 (applicable to stainless steel at potentials more negative than +200 mV vs. SCE) compared to a Cl^-/OH^- ratio of 1 at a depth of 5 cm. The accuracy of these calculations may be limited due to lack of an accurate D_{eff} and uncertainty in estimation of the surface concentration (C_o).^[4,5,39-41] D_{eff} varies with Cl^- and concrete age, concrete quality, and external conditions.^[40] Assumption of a constant C_o may not be appropriate since the value of C_o depends on environmental conditions (in reality, chloride deposition is intermittent and washed away by rainfall). Moreover, an exact calculation of the absolute time until corrosion initiation in service

can not be made because of the variability in road salt deposition and rainfall from one state to another. Therefore, it is difficult to say exactly how long the time until initiation of corrosion would be extended in service with use of stainless steel. Nevertheless, these calculations show that the use of defect free clad rebar could significantly extend the time until initiation of chloride induced corrosion.

CONCLUSIONS

- A universal chloride threshold content for carbon steel has not been adopted due to differences in experimental setup and method of presentation of the results. Regardless, there is consensus that the $[\text{Cl}^-]/[\text{OH}^-]$ molar ratio < 4 for tests conducted in concrete, and $[\text{Cl}^-]/[\text{OH}^-] < 1$ for tests conducted in simulated pore solutions.
- Solid 316LN stainless steel polarized to -200 mV and 0 mV vs. SCE shows a chloride threshold with a $[\text{Cl}^-]/[\text{OH}^-]$ greater than 100 . When polarized to $+200$ mV vs. SCE, the threshold value drops to approximately 24 .
- The chloride threshold for carbon steel was much lower than that of stainless steel at all potentials ($[\text{Cl}^-]/[\text{OH}^-] \leq 1.5$).
- The chloride threshold for carbon steel exhibits a potential dependence. The threshold value is approximately 1 ($[\text{Cl}^-]/[\text{OH}^-]$) at OCP and -200 mV vs. SCE but then drops to less than 0.2 ($[\text{Cl}^-]/[\text{OH}^-]$) at 0 mV and $+200$ mV vs. SCE.
- The chloride threshold for stainless steel clad rebar was found to be strongly dependent on the method of covering the carbon steel core at the cut end of the rebar. At best the chloride threshold is similar to that of solid stainless steel rebar. Conversely, with the cut end left uncovered the chloride threshold is lower than that of carbon steel since the OCP is elevated by approximately 250 mV compared to carbon steel due to galvanic coupling between carbon steel and stainless steel rebar.
- Fickian diffusion calculations show that the observed increase in the chloride threshold for defect free stainless steel rebar may translate to a 50 fold increase in time until initiation of chloride induced corrosion.

REFERENCES

1. J. T. Houston, E. Atimay, and P. M. Ferguson, "Corrosion of Reinforcing Steel Embedded in Structural Concrete." Report No. CFHR-3-5-68-112-1F, Center for Highway Research, University of Texas, Austin, Texas, (1972).
2. J. Ryell, B. S. Richardson, "Cracks in Concrete Bridge Decks and Their Contribution to Corrosion of Reinforcing Steel and Prestressed Cables." Report No. IR51, Ontario Ministry of Transportation and Commission, Ontario, Canada, (1972).
3. K. Tuutti, "Corrosion of steel in concrete." Swedish Cement and Concrete research Institute, Stockholm, 1982.
4. A. Bentour, S. Diamond, N.S. Berke, "Steel Corrosion in Concrete." E & FN Spon, an imprint of Chapman & Hall, 2-6 Boundary Row, London Se1 8HN, UK. 1997.
5. K.E. Curtis, K. Mehta, "A Critical Review of Deterioration of Concrete Due to Corrosion of Reinforcing Steel." Durability of Concrete, Proceedings Fourth CANMET/ACI Int. Conf. Sydney Australia, 1997.
6. L. Li, A.A. Sagues, "Effect of Chloride Concentration on the Pitting and Repassivation Potentials of Reinforcing Steel in Alkaline Solutions." CORROSION '99, NACE International, 1999.
7. A. Rosenberg, C.M. Hansson, C. Andrade, "Mechanisms of Corrosion of Steel in Concrete." Materials Science of Corrosion I, The American Ceramic Society, 1989.
8. D.A. Hausmann, "Steel Corrosion in Concrete. How Does it Occur?" J. Mater. Prot., 1967, pp. 19-23.
9. V. K. Gouda, "Corrosion and Inhibition of Reinforcing Steel." British Corrosion Journal, No. 5, 1970, pp.198-203.
10. M.D.A. Thomas, J.D. Matthews, C.A. Haynes, "Chloride Diffusion and Reinforcement Corrosion in Marine Exposed Concretes Containing PFA." Corrosion of Reinforcement in Concrete, Elsevier, Warwickshire, UK, 1990, pp. 198-212.
11. B.B. Hope, A.K.C. Ip, "Chloride Corrosion Threshold in Concrete," ACI Mater. J., July-August, 1987, pp.306-314.
12. K. Petterson, "Chloride Threshold Value and the Corrosion Rate in Reinforced Concrete." Proceedings of the International Conference on Corrosion Protection of Steel in Concrete, R.N. Swamy (Ed.), Academic Press, Sheffield, 1994, pp. 461.
13. S. Goni, C. Andrade, "Synthetic Concrete Pore Solution Chemistry and Rebar Corrosion Rate in the Presence of Chlorides." Cem. Concr. Res. Vol. 20, 1990, pp. 525-539.

14. P. Lambert, C.L. Page, P.R.W. Vassie, "Investigation of Reinforcement Corrosion. Electrochemical Monitoring of Steel in Chloride Contaminated Concrete." *Mater. Struc.* Vol. 24, 1991, pp. 351-358.
15. K. Petterson, "Chloride Threshold Value and the Corrosion Rate in Reinforced Concrete." CBI Report 2:92, Stockholm, Sweden, 1992.
16. P. Schiessl, W. Breit, "Local Repair Measures at Concrete Structures Damaged by Reinforcement Corrosion." *Proceedings of the Fourth International Symposium on Corrosion of Reinforcement in Concrete Construction*, SCI, Cambridge, 1996, pp. 525-534.
17. C. Andrade, C.L. Page, "Pore Solution Chemistry and Corrosion in Hydrated Cement Systems Containing Chloride Salts." *A Study of Cation Specific Effects*, *Cem Concr. Res.* Vol. 21, 1986, pp.49-53.
18. C. Alonso, C. Andrade, M. Castello, P. Castro, "Chloride Threshold Values to Depassivate Reinforcing Bars Embedded in a Standardized OPC Mortar." *Cem. Concr. Res.* Vol. 30, 2000, 1047-1055.
19. L. Li, A.A. Sagues, "Chloride Corrosion Threshold of Reinforcing Steel in Alkaline Solutions—Open-Circuit Immersion Tests." *Corrosion*, vol. 57, No. 1, 2001, pp. 19-28.
20. C.M. Hansson, B. Sorensen, "The Threshold Concentration of Chloride in Concrete for Initiation of Reinforcement Corrosion." *Corrosion Rates of Steel in Concrete*, N. Berke, V. Whiting (eds.), ASTM Spec. Tech. Pub, 1065, 1988, pp. 3-16.
21. L. Bertolini, F. Bolzoni, T. Pastore, P. Pedferri, "Behaviour of Stainless Steel in Simulated Concrete Pore Solution." *Brit. Corr. J.* Vol. 31, No. 3, 1996, pp. 218-222.
22. V.K. Gouda, W.Y. Halaka, "Corrosion and Corrosion Inhibition of Reinforced Steel." *Brit. Corr. J.* Vol. 5, September 1970, pp. 204-208.
23. ASTM C114-83a, "Standard Method for Chemical Analysis of Hydraulic Cement." American Society for Testing and Materials, Philadelphia, 1983.
24. BS 1881: Part 124: 1988, "The Testing of Hardened Concrete," British Standards Institution, London, 1988.
25. L. Zimmerman, R. Elsener, H. Bohni, "Critical Factors for the Initiation of Rebar Corrosion." Conference paper, Eurocorr '99
26. G.K. Glass, N.R. Buenfeld, "The Influence of Chloride Binding on the Chloride Induced Corrosion Risk in Reinforced Concrete." *Corrosion Science*, Vol. 42, 2000, pp. 329-344.
27. G.K. Glass, N.M. Hassanein, N.R. Buenfeld, *Magazine of Concrete Research*. Vol. 49, 1997, pp. 323.

28. T. Yonezawa, V. Ashworth, R.P.M. Procter, "Pore Solution Composition and Chloride Effects on the Corrosion of Steel in Concrete." *Corrosion*, Vol. 44, No. 7, July 1998, pp. 489-499.
29. Pourbaix, M., "Atlas of Electrochemical Equilibria in Aqueous Solutions." National Association of Corrosion Engineers, Houston TX, 1974.
30. G.K. Glass and N.R. Buenfield, "The Presentation of the Chloride Threshold Level for Corrosion of Steel in Concrete." *Corrosion Science*, Vol. 39, No. 5, 1997, pp. 1001-1013.
31. K.H. Petterson. "Factors Influencing Chloride Induced Corrosion of Reinforced Concrete", *Durability of Building Materials and Components*, Vol. 1, Chapman & Hall, London, 1996, pp. 334-341.
32. O.A. Kayyali, M.N. Haque, "The Ratio of Cl^-/OH^- in Chloride Contaminated Concrete. A Most Important Criterion", *Mag. Concr. Res.* Vol. 47, 1995, pp. 235-242.
33. S.E. Hussain, S.E. Rasheduzzafar, A. Al-Mussallam, A.S. Al-Gahtani, "Factors Affecting Threshold Chloride for Reinforcement Corrosion in Concrete", *Cem. Concr. Res.* Vol. 25, 1995, pp. 1543-1555.
34. M. Thomas, "Chloride Thresholds in Marine Concrete," *Cem. Concr. Res.* Vol. 26, No. 4, 1996, pp. 513-519.
35. R.N. Cox, J.W. Oldfield, "The Long Term Performance of Austenitic Stainless Steel in Chloride Contaminated Concrete." *Corrosion of Reinforcement in Concrete Construction, supplementary Corrosion Protection.* pp. 662-669.
36. J.A. Sedriks. "Corrosion of Stainless Steels." John Wiley & Sons, Inc. 1996.
37. J. Tritthart, *Cem. Concr. Res.* Vol. 19, 1989, pp. 683.
38. M.F. Hurley, J.R. Scully, G. Clemena. "Selected Issues in the Corrosion Resistance of Stainless Steel Clad Rebar." *CORROSION '01* paper #01646, NACE International, 2001.
39. N.S. Berke, M.C. Hicks, "Estimating the Life Cycle of Reinforced Concrete Decks and Marine Piles Using Laboratory Techniques." ASTM STP 1137, "Corrosion Forms and Control for Infrastructure." Victor Chaker (Ed.) Philadelphia, 1992.
40. P.D. Cady, R.E. Weyers, "Predicting Service Life of Concrete Bridge Decks Subject to Reinforcement Corrosion." ASTM STP 1137, "Corrosion Forms and Control for Infrastructure." Victor Chaker (Ed.) Philadelphia, 1992.
41. C. Andrade, C. Alonso, "Progress on Design and Residual Life Calculation with Regard to Rebar Corrosion of Reinforced Concrete." ASTM STP 1276 "Techniques to Assess the Corrosion Activity of Steel Reinforced Concrete Structures." N.S. Berke, E. Escalante, C.K. Nmai, D. Whiting (Eds.) Philadelphia, 1996.

42. ASTM STP 906, "Corrosion Effect of Stray Currents and the Techniques for Evaluating Corrosion of Rebars in Concrete." Victor Chaker (Ed.). Philadelphia, 1985.
43. C.J. Kitowski, H.G. Wheat, "Effect of Chlorides on Reinforcing Steel Exposed to Simulated Concrete Solutions." *Corrosion*, Vol. 53, No. 3, March 1997, pp. 216-226.
44. H.G. Wheat, Z. Eliezer, "Comments on the Identification of a Chloride Threshold in the Corrosion of Steel in Concrete." *Corrosion*, Vol. 43, No. 2, February 1987, pp.126-128.

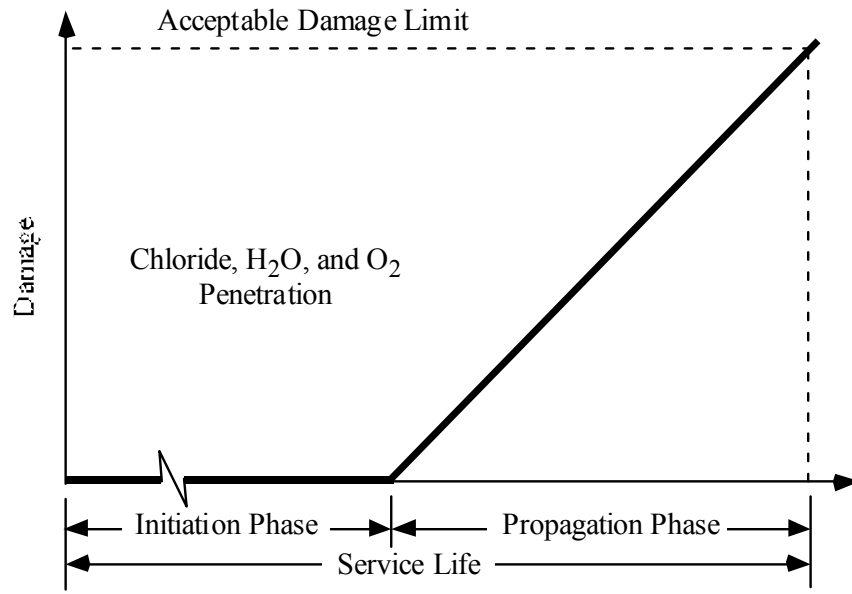


Figure 1. Service life prediction model for reinforced concrete bridges exposed to chloride.

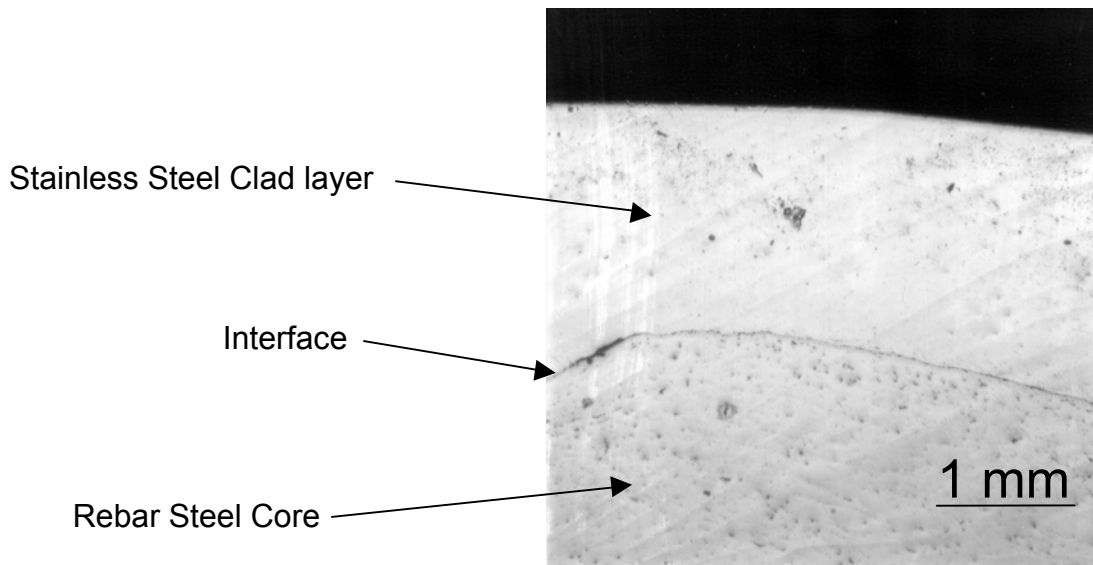


Figure 2. Partial view of a cut end (cut transverse to the bar length) of stainless steel clad rebar, showing the cladding thickness.

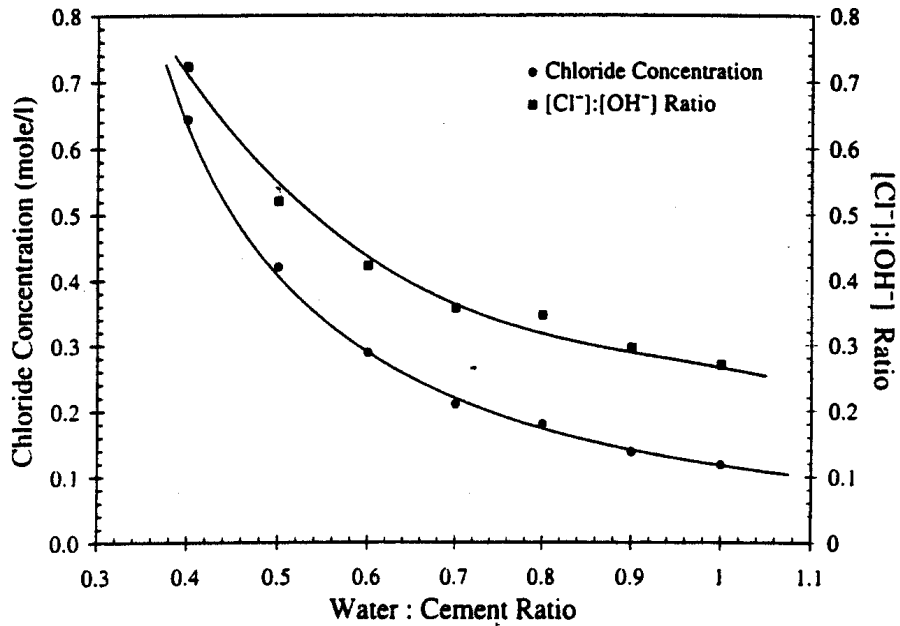


Figure 3. The effect of change in the Water/Cement ratio on the chloride concentration and free $\text{Cl}^-:\text{OH}^-$ molar concentration ratio in OPC cement pastes containing a total of 1% Cl^- added as NaCl .^[37]

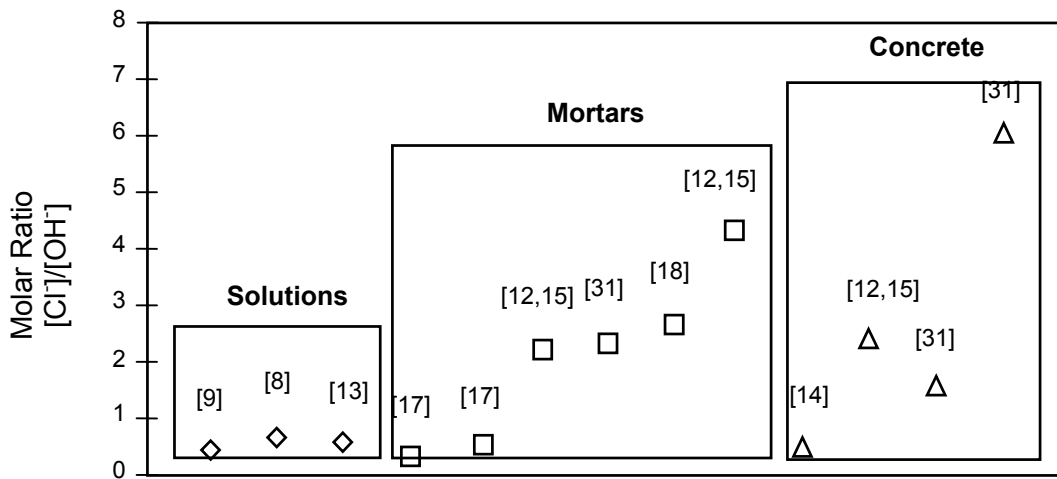


Figure 4. Mean $[\text{Cl}^-:\text{OH}^-]$ molar ratios that represent chloride thresholds for carbon steels for solutions, mortars, and concretes according to different authors, after Alonso et al.^[18] This shows the variability of reported chloride threshold values for carbon steel depending upon the experimental set up used.

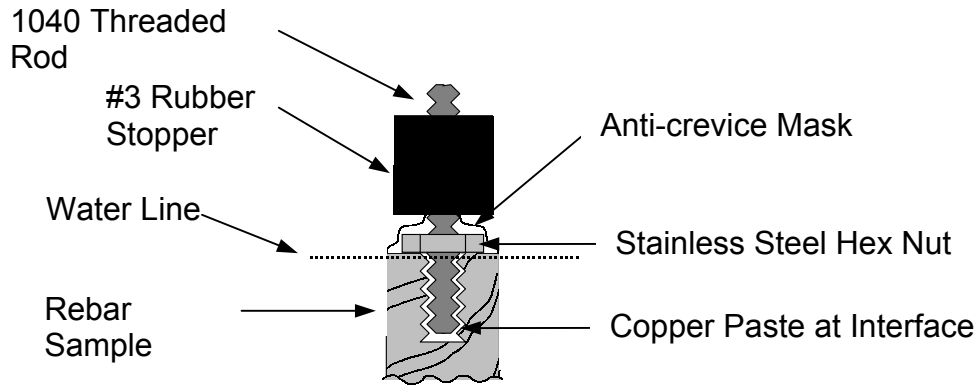


Figure 5. Cross-section schematic view of top of rebar sample designed for chloride threshold testing in a vertical test cell.

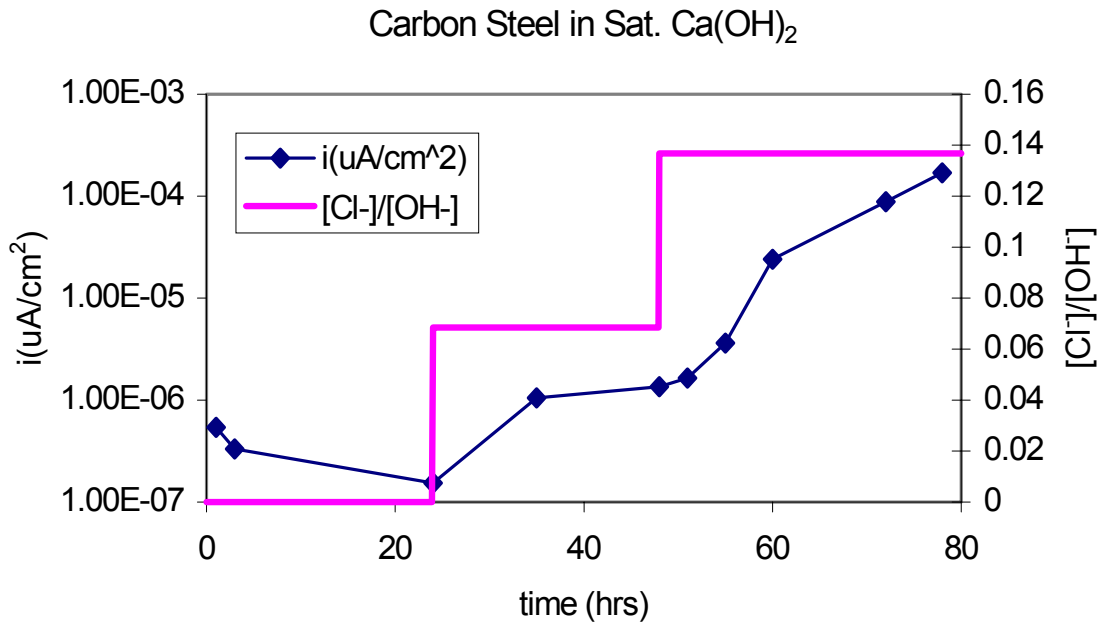


Figure 6. Plot of current density and chloride content vs. time during a chloride threshold test for A615M carbon steel in saturated $\text{Ca}(\text{OH})_2$ at 25°C , potentiostatically polarized to + 200 mV vs. SCE.

Chloride Threshold

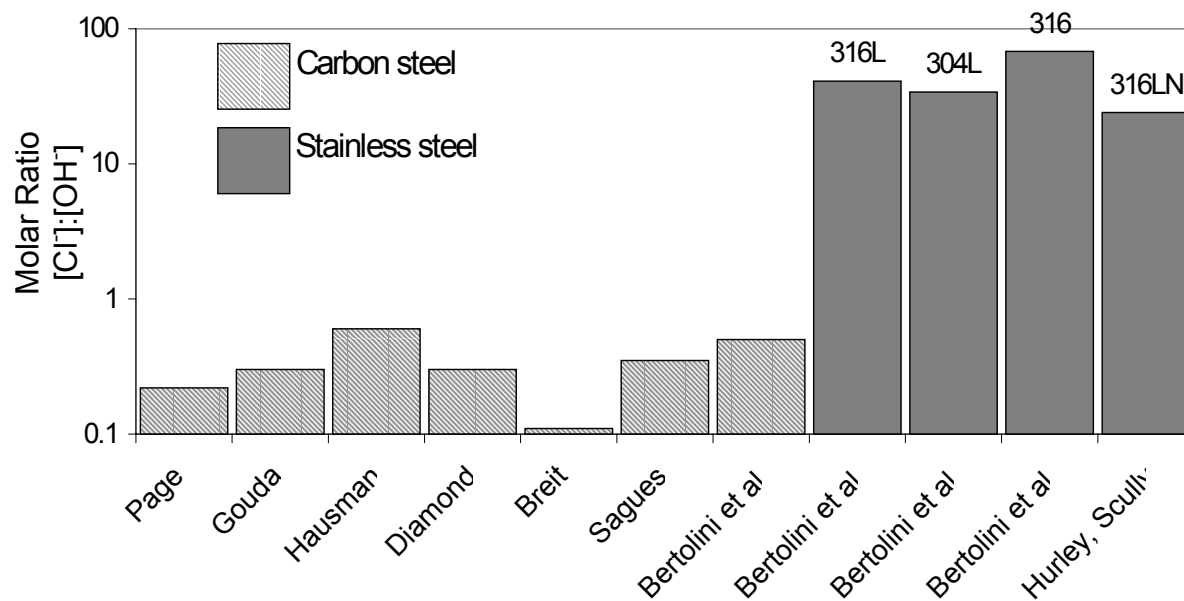


Figure 7. Summary chart showing chloride threshold values for carbon steel and solid stainless steel for various sources. All stainless steel results obtained at +200 mV vs. SCE. Carbon steel tests conducted at free corrosion potential.

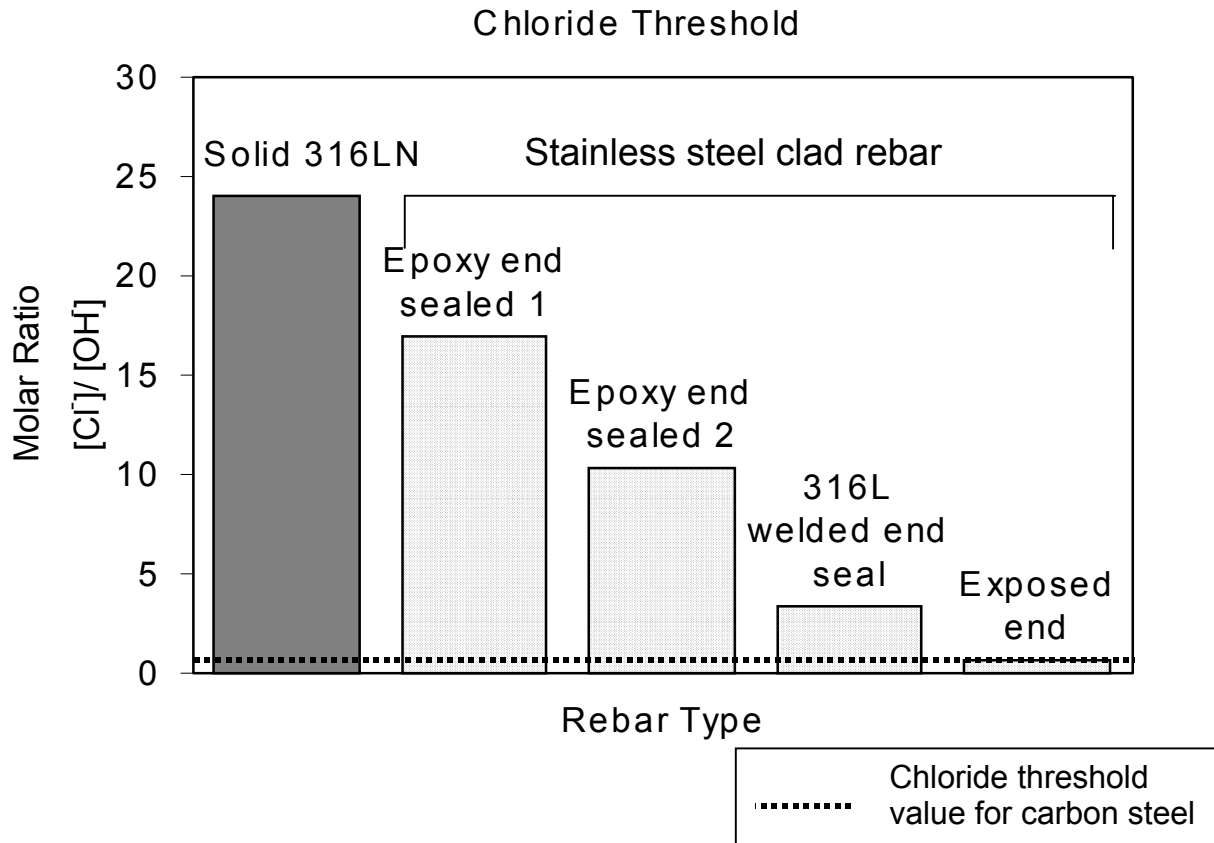


Figure 8. Comparison of chloride threshold values including solid 316LN stainless steel and clad 316L stainless steel rebar. The effect of cut end sealing technique can be seen in the results for the clad bar. The epoxy end sealed values relied on the quality of adhesion and amount of epoxy used. The cut end which was welded showed only a slight increase in chloride threshold compared to that of the exposed cut end owing to weld defects. The chloride threshold for the exposed end was equal to that of carbon steel rebar.

Carbon Steel Core

316L Stainless Steel Clad layer

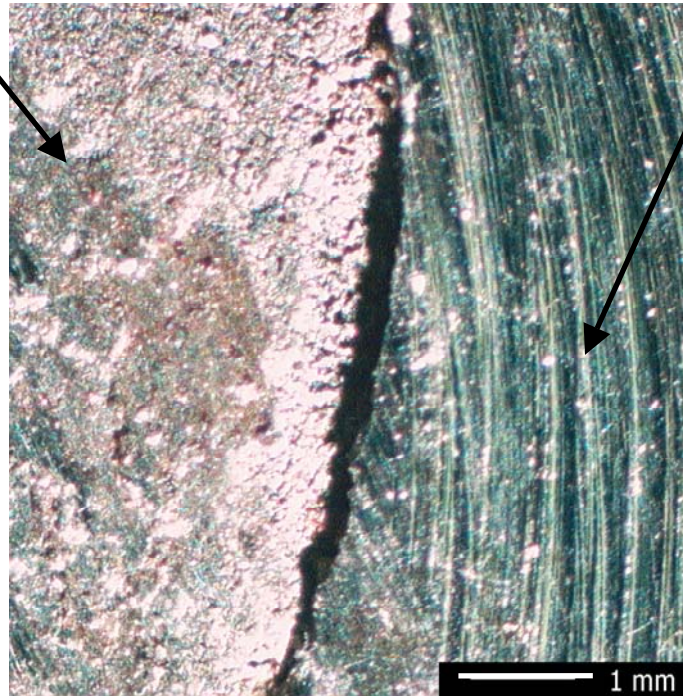


Figure 9. Optical micrograph of stainless steel clad rebar with the cut end epoxy sealed. Micrograph is after testing with the epoxy removed, demonstrating preferential attack on the carbon steel core under the epoxy while the stainless steel cladding shows little evidence of attack.

Chloride Threshold vs. Potentiostatic Hold Potential

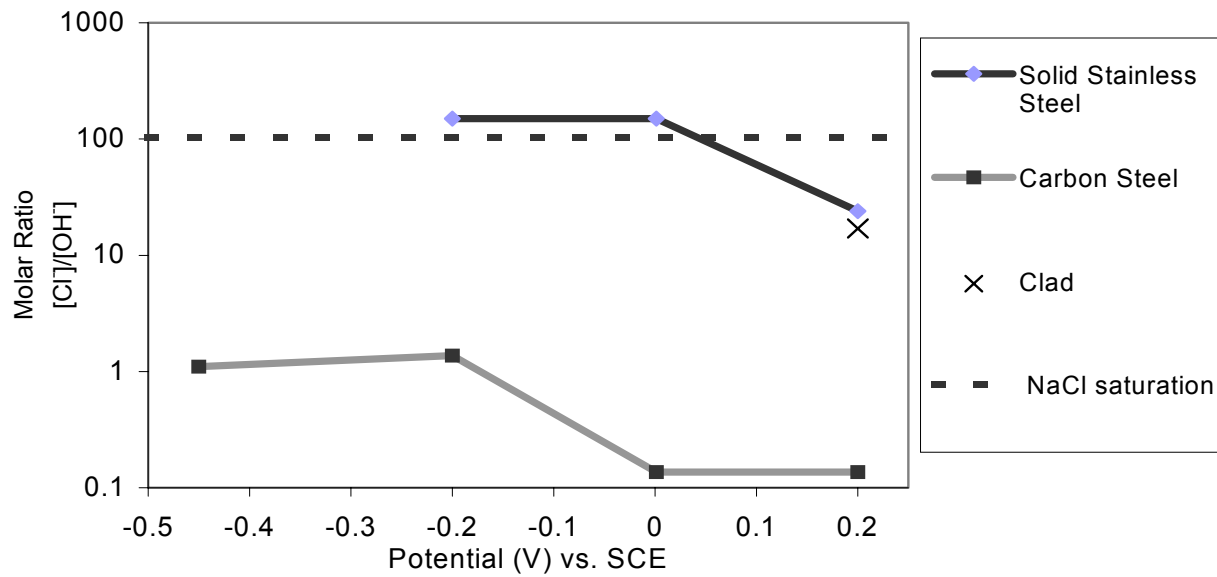


Figure 10. Chloride threshold values as a function of applied potentiostatic hold potential for solid 316LN stainless steel, carbon steel, and 316L stainless steel clad rebar. Tests were conducted in saturated $\text{Ca}(\text{OH})_2$ with NaCl added.

Maximum Open Circuit Potential of Different Rebars in Chloride Contaminated Concrete



Figure 11. Open circuit values for 316LN solid stainless steel, carbon steel, and 316L stainless steel clad rebars in chloride contaminated concrete subjected to wetting-drying cycles.

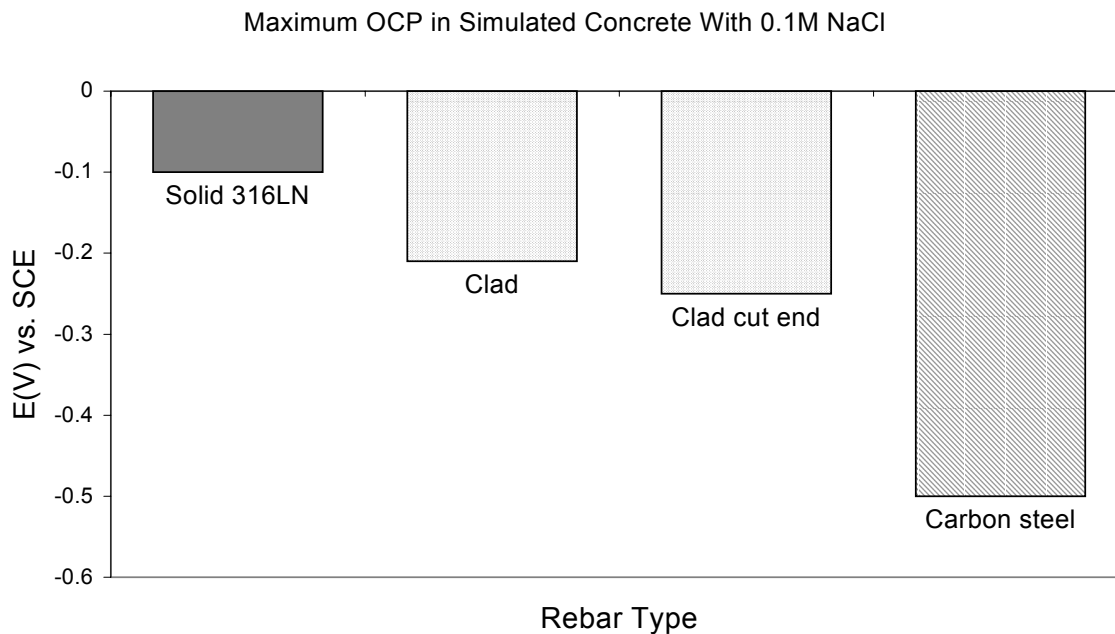


Figure 12. Open circuit values for solid 316LN stainless steel, 316L stainless steel clad, and A615M carbon steel rebar in simulated chloride contaminated concrete environment (Sat. CaOH_2 + 0.1M NaCl). Solid stainless steel is approximately 400 mV more noble than carbon steel. Clad bar with and without the cut end exposed have open circuit potentials greater than -300 mV. The clad bar with the cut end exposed is considerably more noble than the carbon steel.